

Thermodynamic Properties and Plasma Phase Transition in dense Hydrogen

V. S. Filinov ^{*1}, M. Bonitz ², V. E. Fortov ¹, W. Ebeling ³, P. Levashov ¹, and M. Schlanges ⁴

¹ Institute for High Energy Density, Russian Academy of Sciences, Izhorskay 13/19, Moscow 127412, Russia

² Fachbereich Physik, Universität Rostock, D-18051 Rostock, Germany

³ Institut für Physik, Humboldt-Universität Berlin, Invalidenstrasse 110, D-10115 Berlin, Germany

⁴ Fachbereich Physik, Universität Greifswald, D-17489 Greifswald, Germany

Received 16 March 2004, accepted 16 March 2004

Published online 27 August 2004

Key words Plasma phase transition, dense hydrogen, quantum Monte Carlo.

PACS 62.50.+p, 02.70.Rr, 05.30.-d

The internal energy and equation of state of dense hydrogen are investigated by direct path integral Monte Carlo method simulations which are further improved in comparison to our previous results. Data for four isotherms – $T = 10,000\text{K}$, $30,000\text{K}$, $50,000\text{K}$, and $100,000\text{K}$ – are presented. For $T = 10,000\text{K}$ it is shown that the internal energy is lowered due to droplet formation for densities of the order 10^{23}cm^{-3} giving direct support for the existence of a plasma phase transition in megabar hydrogen.

© 2004 WILEY-VCH Verlag GmbH & Co. KGaA, Weinheim

1 Introduction

Strongly correlated Fermi systems and their equilibrium properties at high pressure are of growing importance in many fields, including shock and laser plasmas, astrophysics, solids and nuclear matter, see Refs. [1–7] for an overview. In particular, the thermodynamic properties of *warm dense matter*, such as hydrogen at megabar pressure, are essential for the description of plasmas generated by strong lasers [5], ion beams or free electron lasers. Among the phenomena of particular current interest are the high-pressure compressibility of deuterium [8], metallization of hydrogen [9], Wigner crystallization [10, 11] plasma phase transition etc., which occur in situations where both *interaction and quantum effects* are relevant and a crossover from a neutral system to full ionization takes place. Among the early theoretical papers on dense hydrogen we refer to Wigner/Huntington [12], Abrikosov [13], Ashcroft [14] and Brovman et al. [15] and, concerning the plasma phase transition, see Norman and Starostin [16], Kremp et al. [17], Saumon and Chabrier [18], Schlanges et al. [19], and Ebeling et al. [20]. Further, among the early simulation approaches we refer to several Monte Carlo (MC) calculations, e.g. [21–25]. For a recent overview on the understanding of the hypothetical plasma phase transition, we refer to the paper by Norman [26].

Several methods have been developed to perform quantum MC for dense plasmas. Common to all is the Fermion sign problem: the poor convergence of the simulations for Fermi systems at increasing values of the degeneracy parameter $n\lambda^3$, where n is the density and λ the thermal wavelength (quantum “extension” of the microparticle). First we mention the restricted PIMC method (RPIMC) [27–30]; here special assumptions on the density operator $\hat{\rho}$ are introduced in order to reduce the sum over permutations to even (positive) contributions only. This method crucially depends on the knowledge of the “nodes” of the density operator which can be seen e.g. in the differences of the results computed with free or variational nodes. Furthermore, the presently used nodes apparently exclude the possibility of inhomogeneous plasma configurations, as they would appear in the case of a first order phase transition. Finally, one of us has shown, that this method does not reproduce the correct ideal Fermi gas limit [31].

* Corresponding author: e-mail: filinov@ok.ru, Phone: +07 095 9310719, Fax: +07 095 4857990

For these reasons, the alternative approach of direct fermionic PIMC simulations (DPIMC) is of high value [10, 32], as it avoids all additional assumptions. Obviously, the computational cost is much higher, but the results continue to improve. This method now allows for *direct fermionic path integral Monte Carlo* simulations of dense plasmas in a wide range of densities and temperatures. Using this concept, the pressure and energy of a degenerate strongly coupled hydrogen plasma have been computed [10, 32–36] as well as the pair distribution functions in the region of partial ionization and dissociation [10, 32]. This scheme is rather efficient when the number of time slices (beads) in the path integral is less or equal to 50 and was found to work well for temperatures $k_B T \gtrsim 0.1 Ry$. One of the most striking recent results [35, 37, 38] was the observation of droplet formation in dense hydrogen below $T \lesssim 20,000 K$ which confirmed previous chemical picture results about the plasma phase transition, see above. However, in the region of the instability, the simulations yielded unusually low values for the internal energy. In the present paper, this issue is critically addressed. We present new results which are obtained from an improved treatment of the exchange effects. While these results confirm the formation of droplets, they show that the energy gain of the plasma due to phase separation is much smaller than previously computed because it is partially compensated by an energy increase due to increased Fermionic exchange energy in the high-density droplets.

One difficulty of PIMC simulations is that reliable error estimates are often not available, in particular for strongly coupled degenerate systems. Here, we will make a comparison with two independent analytical methods. The first is the method of an effective ion-ion interaction potential (EIIP) which has previously been developed for application to simple solid and liquid metals [15] and which was adopted in [36] to dense hydrogen. The second is the method of Padé approximations in combination with Saha equations, i.e. the chemical picture (PACH) [3].

2 Brief summary of the direct path integral Monte Carlo simulations

The main idea of DPIMC simulations is to perform first-principle calculations which avoid any additional assumptions. In particular, no assumptions on the chemical composition or the type of bound states which exist in the system or on the homogeneity of the plasma are made. This is crucial in the region of the Mott transition where the plasma composition, the degree of ionization and dissociation changes rapidly in a narrow density interval. Thus, we start from the basic plasma particles: electrons and ions. Feynmans path integral concept together with Monte Carlo methods “automatically” accounts for bound state formation and ionization and dissociation. Furthermore, in contrast to a chemical picture, no restrictions on the type of chemical species are made and the appearance of complex aggregates such as molecular ions or clusters of several atoms are fully included. On the other hand, the simulations are expected to become increasingly difficult at high density where the electron degeneracy is large due to the Fermion sign problem.

Let us briefly outline the idea of our DPIMC scheme. All thermodynamic properties of a two-component plasma are defined by the partition function Z which, for the case of N_e electrons and N_p protons, is given by

$$Z(N_e, N_p, V, \beta) = \frac{Q(N_e, N_p, \beta)}{N_e! N_p!},$$

$$\text{with } Q(N_e, N_p, \beta) = \sum_{\sigma} \int_V dq dr \rho(q, r, \sigma; \beta), \quad (1)$$

where $\beta = 1/k_B T$. The exact density matrix is, for a quantum system, in general, not known but can be constructed using a path integral representation [21, 39–41],

$$\int_V dR^{(0)} \sum_{\sigma} \rho(R^{(0)}, \sigma; \beta) = \int_V dR^{(0)} \dots dR^{(n)} \rho^{(1)} \cdot \rho^{(2)} \dots \rho^{(n)}$$

$$\times \sum_{\sigma} \sum_P (\pm 1)^{\kappa_P} \mathcal{S}(\sigma, \hat{P} \sigma') \hat{P} \rho^{(n+1)}, \quad (2)$$

where $\rho^{(i)} \equiv \rho(R^{(i-1)}, R^{(i)}; \Delta\beta) \equiv \langle R^{(i-1)} | e^{-\Delta\beta \hat{H}} | R^{(i)} \rangle$ and $\Delta\beta \equiv \beta/(n+1)$. Further, \hat{H} is the Hamilton operator, $\hat{H} = \hat{K} + \hat{U}_c$, containing kinetic and potential energy contributions, \hat{K} and \hat{U}_c , respectively, with $\hat{U}_c = \hat{U}_c^p + \hat{U}_c^e + \hat{U}_c^{ep}$ being the sum of the Coulomb potentials between protons (p), electrons (e) and

electrons and protons (ep). Further, σ comprises all particle spins, and the particle coordinates are denoted by $R^{(i)} = (q^{(i)}, r^{(i)}) \equiv (R_p^{(i)}, R_e^{(i)})$, for $i = 1, \dots, n+1$, $R^{(0)} \equiv (q, r) \equiv (R_p^{(0)}, R_e^{(0)})$, and $R^{(n+1)} \equiv R^{(0)}$ and $\sigma' = \sigma$. This means, the particles are represented by fermionic loops with the coordinates (beads) $[R] \equiv [R^{(0)}; R^{(1)}; \dots; R^{(n)}; R^{(n+1)}]$, where q and r denote the electron and proton coordinates, respectively. The spin gives rise to the spin part of the density matrix \mathcal{S} , whereas exchange effects are accounted for by the permutation operator \hat{P} , which acts on the electron coordinates and spin projections, and the sum over the permutations with parity κ_P . In the fermionic case (minus sign), the sum contains $N_e!/2$ positive and negative terms leading to the notorious sign problem. Due to the large mass difference of electrons and ions, the exchange of the latter is not included.

To compute thermodynamic functions, the logarithm of the partition function has to be differentiated with respect to thermodynamic variables. In particular, the internal energy E follows from Q by

$$\beta E = -\beta \partial \ln Q / \partial \beta, \quad (3)$$

This leads to the following result (for details, cf. [33]),

$$\begin{aligned} \beta E = & \frac{3}{2}(N_e + N_p) + \frac{1}{Q} \frac{1}{\lambda_p^{3N_p} \Delta \lambda_e^{3N_e}} \sum_{s=0}^{N_e} \int dq dr d\xi \rho_s(q, [r], \beta) \times \\ & \left\{ \sum_{p<t}^{N_p} \frac{\beta e^2}{|q_{pt}|} + \sum_{l=0}^n \left[\sum_{p<t}^{N_e} \frac{\Delta \beta e^2}{|r_{pt}^l|} + \sum_{p=1}^{N_p} \sum_{t=1}^{N_e} \Psi_l^{ep} \right] \right. \\ & \left. + \sum_{l=1}^n \left[- \sum_{p<t}^{N_e} C_{pt}^l \frac{\Delta \beta e^2}{|r_{pt}^l|^2} + \sum_{p=1}^{N_p} \sum_{t=1}^{N_e} D_{pt}^l \frac{\partial \Delta \beta \Phi^{ep}}{\partial |x_{pt}^l|} \right] - \frac{1}{\det |\psi_{ab}^{n,1}|_s} \frac{\partial \det |\psi_{ab}^{n,1}|_s}{\partial \beta} \right\}, \quad (4) \\ & \text{with } C_{pt}^l = \frac{\langle r_{pt}^l | y_{pt}^l \rangle}{2|r_{pt}^l|}, \quad D_{pt}^l = \frac{\langle x_{pt}^l | y_p^l \rangle}{2|x_{pt}^l|}, \quad \Delta \lambda_e^2 = 2\pi \hbar^2 \Delta \beta / m_e, \end{aligned}$$

and $\Psi_l^{ep} \equiv \Delta \beta \partial [\beta' \Phi^{ep}(|x_{pt}^l|, \beta')]/\partial \beta' |_{\beta'=\Delta \beta}$ contains the electron-proton Kelbg potential Φ^{ep} , cf. Eq. (6) below. Here, $\langle \dots | \dots \rangle$ denotes the scalar product, and q_{pt} , r_{pt} and x_{pt} are differences of two coordinate vectors: $q_{pt} \equiv q_p - q_t$, $r_{pt} \equiv r_p - r_t$, $x_{pt} \equiv r_p - q_t$, $r_{pt}^l = r_{pt} + y_{pt}^l$, $x_{pt}^l \equiv x_{pt} + y_p^l$ and $y_{pt}^l \equiv y_p^l - y_t^l$, with $y_a^n = \Delta \lambda_e \sum_{k=1}^n \xi_a^{(k)}$. Here we introduced dimensionless distances between neighboring vertices on the loop, $\xi^{(1)}, \dots, \xi^{(n)}$, thus, explicitly, $[r] \equiv [r; y_e^{(1)}; y_e^{(2)}; \dots]$. Further, the density matrix ρ_s in Eq. (4) is given by

$$\rho_s(q, [r], \beta) = C_{N_e}^s e^{-\beta U(q, [r], \beta)} \prod_{l=1}^n \prod_{p=1}^{N_e} \phi_{pp}^l \det |\psi_{ab}^{n,1}|_s, \quad |\psi_{ab}^{n,1}|_s \equiv \left| e^{-\frac{\pi}{\Delta \lambda_e^2} |(r_a - r_b) + y_a^n|^2} \right|_s. \quad (5)$$

where $U(q, [r], \beta) = U_c^p(q) + \{U^e([r], \Delta \beta) + U^{ep}(q, [r], \Delta \beta)\}/(n+1)$ and $\phi_{pp}^l \equiv e^{-\pi |\xi_p^{(l)}|^2}$. We point out that the density matrix (5) does not contain an explicit sum over the permutations and thus no sum of terms with alternating sign. Instead, the whole exchange problem is contained in a single exchange matrix $|\psi_{ab}^{n,1}|_s$, which, as a result of the spin summation, carries a subscript s denoting the number of electrons having the same spin projection.

The potential Φ^{ab} appearing in Eq. (4) is an effective quantum pair interaction between two charged particles immersed into a weakly degenerate plasma. It has been derived by Kelbg and co-workers [42, 43] who showed that it contains quantum effects exactly in first order in the coupling parameter Γ ,

$$\Phi^{ab}(|\mathbf{r}_{ab}|, \Delta \beta) = \frac{e_a e_b}{\lambda_{ab} x_{ab}} \left\{ 1 - e^{-x_{ab}^2} + \sqrt{\pi} x_{ab} [1 - \text{erf}(x_{ab})] \right\}, \quad (6)$$

where $x_{ab} = |\mathbf{r}_{ab}|/\lambda_{ab}$, and we underline that the Kelbg potential is finite at zero distance. We mention recent improvements of this potential [44] which allow to extend it into the region of moderate coupling and partial ionization. These results will be used in future work.

The structure of Eq. (4) is obvious: we have separated the classical ideal gas part (first term). The ideal quantum part in excess of the classical one and the correlation contributions are contained in the integral term, where

the second line results from the ionic correlations (first term) and the e-e and e-i interaction at the first vertex (second and third terms respectively). Thus, Eq. (4) contains the important limit of an ideal quantum plasma in a natural way. The third line is due to the further electronic vertices and the explicit temperature dependence [in Eq. (4)] and volume dependence (in the corresponding equation of state result) of the exchange matrix, respectively. The main advantage of Eq. (4) is that the explicit sum over permutations has been converted into the spin determinant which can be computed very efficiently using standard linear algebra methods. Furthermore, each of the sums in curly brackets in Eq. (4) is bounded as the number of vertices increases, $n \rightarrow \infty$. The error of the total expression is of the order of $1/n$. Thus, expression (4) and the analogous result for the equation of state are well suited for numerical evaluation using standard Monte Carlo techniques, e.g. [21, 25].

In our Monte Carlo scheme we used three types of steps, where either electron or proton coordinates, r_i or q_i or individual electronic beads $\xi_i^{(k)}$ were moved until convergence of the calculated values was reached. Our procedure has been extensively tested. In particular, we found from comparison with the known analytical expressions for pressure and energy of an ideal Fermi gas that the Fermi statistics is very well reproduced with a limited number of particles, $N \lesssim 100$, and beads, $n \lesssim 20$, [10, 32, 33].

3 Numerical Results. Comparison of the analytical and simulation data

Let us now come to the numerical results. The path integral representation for the N-particle density operator discussed above allows for *direct fermionic path integral Monte Carlo* (DPIMC) simulations of dense plasmas in a wide range of densities and temperatures. Using this concept, the pressure, energy and the pair distribution functions of a degenerated strongly coupled hydrogen plasma have been computed in the region of partial ionization and dissociation [10, 33–37].

Here, we present improved results for the pressure and internal energy of dense hydrogen. In Figs. 1–4 we present isotherms for the temperatures 10, 000, 30, 000, 50, 000, 100, 000K. First, in all figures we observe the familiar general behavior of the thermodynamic functions of a nonideal plasma: the formation of a pressure and energy minimum (where the energy may become negative) at intermediate densities (around 10^{23}cm^{-3}), which is due to the (overall attractive) Coulomb correlations leading in particular to formation of atoms and molecules. At larger densities energy and pressure rapidly increase which is a consequence of electron degeneracy effects: increasing overlap of the electron wave functions leads to a break up of bound states (Mott effect) and to increased exchange energy. These quantum contributions start to become important around the energy minimum and thus strongly influence the lowest value of the total energy per $2N$ protons on the isotherms. In our previous calculations, this value was unexpectedly low, around $1Ry$ for $T=10,000K$. We, therefore, did a careful analysis of these results and improved the treatment of the electron exchange. In previous calculations, exchange effects were only computed between particles inside the Monte Carlo cell. However, with increasing $n\lambda^3$ also the ratio of the thermal electron wave length to the size of Monte Carlo cell increases. When this ratio approaches one, of course, exchange effects between electrons in the main MC cell and their images in the neighbor cells have to be included. In the present calculations we take into account the exchange interaction of electrons from neighbor Monte Carlo cells, namely first from the nearest neighbor cells ($3^3 - 1$), then from the next neighbors $5^3 - 1$ and so on. These improved calculations were first tested for an ideal plasma and then for a nonideal hydrogen plasma, see Figs. 2–4. The agreement with the known analytical results for an ideal plasma is now very good up to densities of the order of $5 \cdot 10^{23}\text{cm}^{-3}$.

With the improved treatment of electronic exchange, the lowest value for the energies increases significantly. For $T=10,000K$ the minimum of the energy per $2N$ protons is now around $0.6Ry$ with an average magnitude of the fluctuations (due to the observed instability) of $0.4Ry$. At the same time, the formation of clusters in this region found in our previous calculations [37, 45] is reproduced by the present results, confirming our conclusion about the plasma phase transition.

Let us now compare the results from DPIMC method, the method of an effective ion-ion interaction potential (EIIP [36]), Padé approach within the chemical picture (PACH [3]) and density functional results for $T=10,000K$ (DFT [46]). These methods are constructed in a way that they correctly reproduce the known analytical behavior at very high densities, $n > 10^{24}\text{cm}^{-3}$ where they agree well with each other. For us the densities below this range are of interest. Here, as we mentioned above, atom and molecule formation is becoming important, and the DFT and EIIP methods (in their present form) are becoming increasingly unreliable. In contrast, the

presented PACH results include bound states approximately. Further, the PACH and DFT methods are assuming homogeneous density distributions and thus cannot describe phase separation. Interestingly, at $T = 10,000\text{K}$ and $10^{23}\text{cm}^{-3} \leq n \leq 10^{24}\text{cm}^{-3}$, both the Pade and EIIP methods yield unstable results for the thermodynamic functions which is a clear indication for the existence of a first order phase transition. Xu and Hansen [46] too observed strong fluctuations in their density functional calculations below $r_s = 1.5$ which they found to strongly resemble precursors of a phase transition. Let us now compare the DPIMC simulations to the results of RPIMC simulations of Militzer et al. [30]. We found excellent quantitative agreement between the two independent quantum Monte Carlo methods above $T = 50,000\text{K}$, see for example the point for $T = 62,500\text{K}$ in Fig. 4.a, and also Ref. [33] where a more extensive comparison is given. At lower temperatures the DPIMC results for the energy are mainly lower than the RPIMC results. In particular, our results for the energy minimum are lower which is due to droplet formation, apparently excluded by the fixed node approximation in the RPIMC simulations. We mention that the same effects are observed in our DPIMC simulations of electron-hole plasmas under similar conditions [35, 45] for which droplet formation is well established and observed experimentally three decades ago [47].

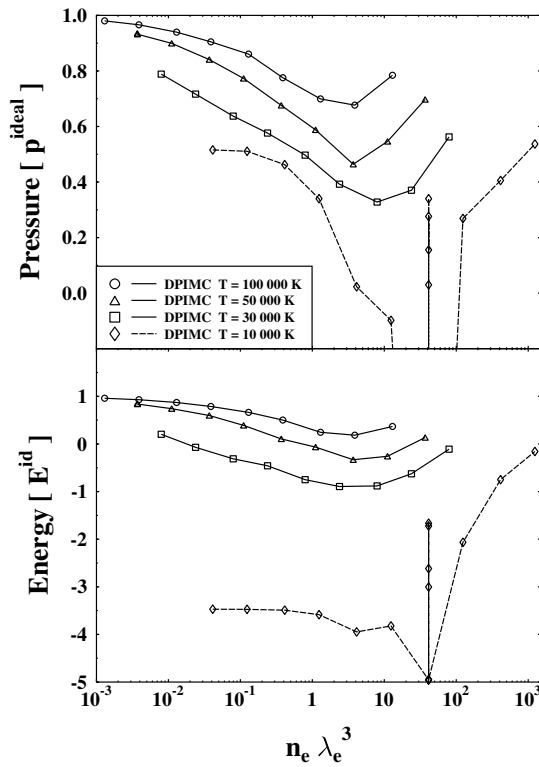


Fig. 1 Pressure and energy isotherms of dense hydrogen vs. degeneracy parameter (λ_e is the electron thermal De-Broglie wavelength). For $T = 10,000\text{K}$, in the range of $10 \lesssim n_e \lambda_e^3 \lesssim 100$, due to droplet formation, strong fluctuations of the energy occur, whereas the simulation results for the pressure do not converge.

4 Discussion

This work is devoted to the investigation of the pressure and the total energy of warm dense plasmas in the temperature region between 10,000 and 100,000K. We presented new results for high-density plasmas and

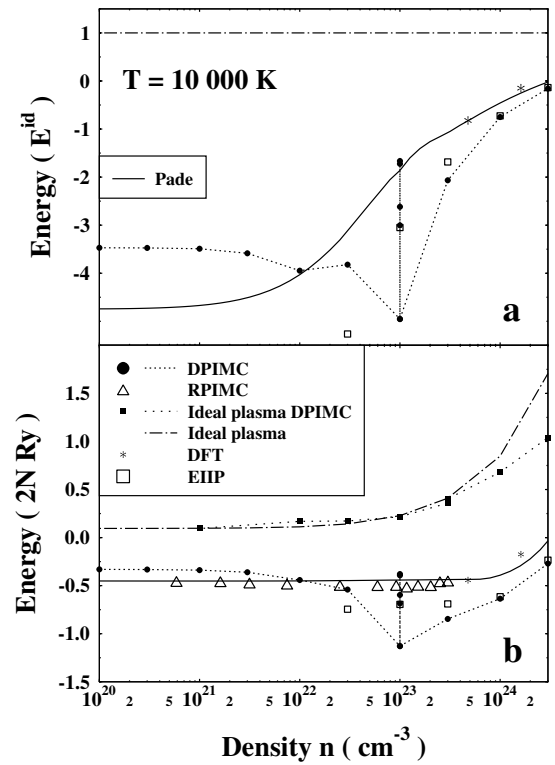


Fig. 2 Internal energy of hydrogen for $T = 10,000\text{K}$, a) normalized to the energy of a noninteracting electron-proton system and b) in units of $2N$ -Rydberg. The curves show results of an effective ion-ion interaction potential method (“EIIP”), PACH-calculations (“Pade”), our Monte Carlo simulations (“DPIMC”), density functional theory (“DFT”) [46] and restricted PIMC data (“RPIMC”) of Militzer et al. [29, 30]. Further, we compare our DPIMC results for an ideal plasma with the analytical result.

compare them with results based on several theoretical methods, namely the theory of an effective ion-ion potential (EIIP), the Padé formalism within the chemical picture, density functional theory and the restricted path integral Monte Carlo method (RPIMC). From these comparisons we conclude that the considered theoretical approaches – DPIMC, RPIMC, PACH, EEIP and DFT – are in good overall agreement with each other for a fully ionized hydrogen plasma in the high density region. On the other hand, our DPIMC simulations agree well with the available RPIMC data, cf. Figs. 2 - 4 and Ref. [33], for temperatures above 50,000K. This agreement over a broad range of parameters is certainly remarkable since the plasma is far outside the perturbative regime: it is strongly correlated and the electrons are degenerate, and the two simulations are essentially independent.

In addition, at low temperature, we observe deviations in the region of the energy minimum, around $n = 10^{23} \text{cm}^{-3}$, where the DPIMC data are substantially lower. Our analysis revealed that these deviations are due to droplet formation found in the DPIMC simulations which are not included in the other methods. Our improved treatment of exchange effects which included exchange with particles of the neighboring MC cells has reduced these differences. Our energies are now close to those of the molecular ground state.

Finally, for completeness we mention that, at very high density of the order of 10^{26}cm^{-3} , our DPIMC simulations revealed ordering of protons into a strongly correlated fluid and the onset of the formation of a proton Wigner crystal [10, 45]. These interesting physical effects in high pressure hydrogen are of relevance for many astrophysical systems, but also for many laboratory experiments, including ultracold degenerate trapped ions and laser plasmas.

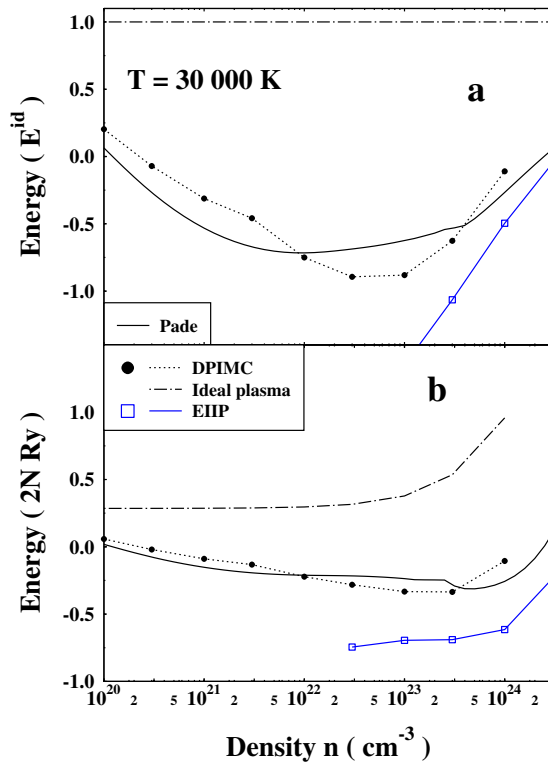


Fig. 3 Same as Fig. 2, but for $T = 30,000 \text{K}$.

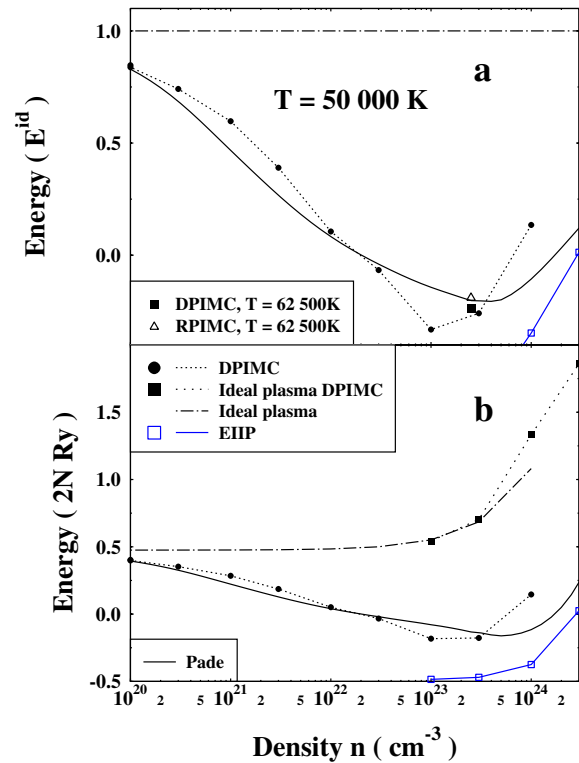


Fig. 4 Same as Fig. 2, but for $T = 50,000 \text{K}$.

Acknowledgements We acknowledge stimulating discussions with H.E. DeWitt, W.D. Kraeft, D. Kremp, B. Militzer and R. Redmer. This work has been supported by the Deutsche Forschungsgemeinschaft (BO-1366/3) and by grants for CPU time at the NIC Jülich and the Rostock Linux-Cluster “Fermion”.

References

- [1] G. Kalman (ed.) *Strongly Coupled Coulomb Systems*, Pergamon Press (1998).

- [2] W.D. Kraeft, M. Schlanges (eds.) *Proceedings of the International Conference on Strongly Coupled Plasmas*, World Scientific, Singapore (1996).
- [3] W.D. Kraeft, D. Kremp, W. Ebeling, G. Röpke, *Quantum Statistics of Charged Particle Systems*, Akademie-Verlag Berlin (1986).
- [4] M. Bonitz, "Quantum Kinetic Theory", B.G. Teubner, Stuttgart/Leipzig (1998).
- [5] H. Haberland, M. Schlanges, W. Ebeling (eds.): Proc. 10th Int. Workshop on the Physics of Nonideal Plasmas, Contrib. Plasma Phys. **41**, No.2-3 (2001).
- [6] M. Bonitz (ed.), "Progress in Nonequilibrium Greens Functions", World Scientific Publ., Singapore (2000); M. Bonitz, D. Semkat (eds.), "Progress in Nonequilibrium Greens Functions II", World Scientific Publ., Singapore (2003).
- [7] M. Bonitz, D. Semkat, A. Filinov, V. Golubnychi, D.O. Gericke, M.S. Murillo, V. Filinov, W. Hoyer, S.W. Koch, J. Phys. A: Math. Gen. **36**, 5921 (2003).
- [8] L.B. Da Silva et al., Phys. Rev. Lett. **78**, 483 (1997).
- [9] S.T. Weir, A.C. Mitchell, W.J. Nellis, Phys. Rev. Lett. **76**, 1860 (1996).
- [10] V.S. Filinov, M. Bonitz, V.E. Fortov, JETP Letters **72**, 245 (2000).
- [11] A.V. Filinov, M. Bonitz, Yu.E. Lozovik, Phys. Rev. Lett. **86**, 3851 (2001).
- [12] E.P. Wigner, H.B. Huntington, J. Chem. Phys. **3**, 764 (1935).
- [13] A.A. Abrikosov, JETP (Sov.Phys. - JETP), **39**, 1798 (1960); **41**, 565 (1961); **45**, 2038 (1962).
- [14] N.W. Ashcroft, D. Stroud, in Solid State Physics, ed. by H. Ehrenreich, F. Seitz, D. Turnbull (Academic N.Y.), v. 33, p.1. N.W. Ashcroft, Phys.Rev.Lett. **21**, 1748 (1968).
- [15] E.G. Brovman, Yu. Kagan, A. Kholas, JETP (Sov.Phys. - JETP) **61**, 2429 (1971).
- [16] G.E. Norman, A.N. Starostin, Teplofiz. Vys. Temp. **6**, 410 (1968); **8**, 413 (1970), [Sov. Phys. High Temp. **6**, 394 (1968); **8**, 381 (1970)].
- [17] P. Haronska, D. Kremp, M. Schlanges, Wiss. Z. Universität Rostock **98**, 1 (1987).
- [18] D. Saumon, G. Chabrier, Phys. Rev. A **44**, 5122 (1991).
- [19] M. Schlanges, M. Bonitz, A. Tschtschjan, Contrib. Plasma Phys. **35**, 109 (1995).
- [20] W. Ebeling, W.D. Kraeft, D. Kremp, "Theory of bound states and ionization equilibrium in plasmas and solids". Akademie-Verlag Berlin 1976; Russ. Transl. Mir Moscow 1979.
- [21] V.M. Zamalin, G.E. Norman, V.S. Filinov, *The Monte Carlo Method in Statistical Thermodynamics*, (Nauka, Moscow) 1977 (in Russian); B.V. Zelener, G.E. Norman, V.S. Filinov, *Perturbation Theory and Pseudopotential in Statistical Thermodynamics*, (Nauka, Moscow) 1981 (in Russian).
- [22] J.-P. Hansen, P. Viennefosse, Phys. Lett. A, **53**, 187 (1975); S. Galam, J.P. Hansen, Phys. Rev. A **14**, 816 (1976).
- [23] H.E. De Witt, in *Strongly Coupled Plasmas*, ed. G. Kalman, P. Carini (Plenum N.Y.), 1978.
- [24] D. Klakow, C. Toepffer, P.-G. Reinhard, Phys. Lett. A **192**, 55 (1994); J. Chem. Phys. **101**, 10766 (1994).
- [25] K. Binder, G. Cicotti (eds.), *The Monte Carlo and Molecular Dynamics of Condensed Matter Systems*, SIF, Bologna 1996.
- [26] G.E. Norman, Contrib. Plasma Phys. **41**, 127 (2001).
- [27] D.M. Ceperley, in Ref. [25], pp. 447-482.
- [28] D.M. Ceperley, Rev. Mod. Phys. **65**, 279 (1995).
- [29] B. Militzer, E.L. Pollock, Phys. Rev. E **61**, 3470 (2000).
- [30] B. Militzer, D.M. Ceperley, Phys. Rev. Lett. **85**, 1890 (2000).
- [31] V.S. Filinov, J. Phys. A **34**, 1665 (2001).
- [32] V.S. Filinov, V.E. Fortov, M. Bonitz, D. Kremp, Phys. Lett. A **274**, 228 (2000).
- [33] V.S. Filinov, M. Bonitz, W. Ebeling, V.E. Fortov, Plasma Phys. Contr. Fusion **43**, 743 (2001).
- [34] P.R. Levashov, V.S. Filinov, V.E. Fortov, M. Bonitz, Thermodynamic Properties of Nonideal Strongly Degenerate Hydrogen Plasma in: CP620, Shock Compression of Condensed Matter - 2001, Eds. M.D. Furnish, N.N. Thadhani, Y. Horie, American Institute of Physics, p. 119-124, (2002); P.R. Levashov, V.S. Filinov, V.E. Fortov, M. Bonitz, Authors' Reply in: Shock Compression of Condensed Matter - 2001., Eds. M.D. Furnish, N.N. Thadhani, and Y. Horie, American Institute of Physics, p. 125-126, (2002).
- [35] V.S. Filinov, M. Bonitz, P.R. Levashov, V.E. Fortov, W. Ebeling, M. Schlanges, S.W. Koch, J. Phys. A: Math. Gen. **36**, 6069 (2003).
- [36] S.A. Trigger, W. Ebeling, V.S. Filinov, V.E. Fortov, M. Bonitz, JETP, v. 96 N. 3, 465-479, (2003) (ArXiv: physics/0110013).
- [37] V.S. Filinov, V.E. Fortov, M. Bonitz, P.R. Levashov, JETP Lett. **74**, 384 (2001) [Pis'ma v ZhETF **74**, 422 (2001)].
- [38] M. Bonitz, Physik Journal No. 7/8, p. 69 (2002).
- [39] R.P. Feynman, A.R. Hibbs, *Quantum mechanics and path integrals*, McGraw-Hill, New York 1965.
- [40] V.S. Filinov, High Temperature **13**, 1065 (1975) and **14**, 225 (1976).
- [41] B.V. Zelener, G.E. Norman, V.S. Filinov, High Temperature **13**, 650, (1975).
- [42] G. Kelbg, Ann. Physik, **12**, 219 (1963); **13**, 354; **14**, 394 (1964).
- [43] W. Ebeling, H.J. Hoffmann, G. Kelbg, Contr. Plasma Phys. **7**, 233 (1967) and references therein.
- [44] A. Filinov, M. Bonitz, W. Ebeling, J. Phys. A: Math. Gen. **36** (2003).
- [45] M. Bonitz et al., J.Phys.A: Math. Gen. **36**, 5921 (2003).
- [46] H. Xu, J.P. Hansen, Phys. Rev. E **57**, 211 (1998).
- [47] For reviews, see e.g. *Electron-hole droplets in semiconductors*, C.D. Jeffries, L.V. Keldysh (eds.), Nauka, Moscow (1988); J.C. Hensel, T.G. Phillips, G.A. Thomas, Solid State Phys. vol. **32**, p. 88 (1977).